

Two-body relaxation of spin-polarized fermions in reduced dimensionalities near a p -wave Feshbach resonance

D. V. Kurlov^{1,2} and G. V. Shlyapnikov^{1,2,3,4,5}

¹*Van der Waals-Zeeman Institute, Institute of Physics, University of Amsterdam, Science Park 904, 1098 XH Amsterdam, The Netherlands*

²*LPTMS, CNRS, Univ. Paris-Sud, Université Paris-Saclay, 91405 Orsay, France*

³*SPEC, CEA, CNRS, Univ. Paris-Saclay, CEA Saclay, Gif sur Yvette 91191, France*

⁴*Russian Quantum Center, Novaya Street 100, Skolkovo, Moscow Region 143025, Russia*

⁵*State Key Laboratory of Magnetic Resonance and Atomic and Molecular Physics, Wuhan Institute of Physics and Mathematics, Chinese Academy of Sciences, Wuhan 430071, China*

We study inelastic two-body relaxation in a spin-polarized ultracold Fermi gas in the presence of a p -wave Feshbach resonance. It is shown that in reduced dimensionalities, especially in the quasi-one-dimensional case, the enhancement of the inelastic rate constant on approach to the resonance is much weaker than in three dimensions. This may open promising paths for obtaining novel many-body states.

I. INTRODUCTION

Recent progress in the field of ultracold atomic quantum gases opened fascinating prospects to explore novel quantum phases in the systems of degenerate fermions with p -wave interactions, for instance two-dimensional (2D) unconventional superfluidity [1], non-Abelian Majorana modes [2, 3], and itinerant ferromagnetism [4–7]. Even though the p -wave interactions between cold fermions are much weaker than the s -wave interactions, Feshbach resonances allow one to tune the strength and the character of the interactions. However, in the vicinity of such resonances various inelastic collisional processes play a crucial role, resulting in a lifetime of the order of milliseconds at common densities. These are three-body recombination and, for fermionic atoms in an excited hyperfine state, two-body relaxation [8–13].

In this paper we show that in the quasi-2D and quasi-1D geometries the enhancement of two-body inelastic relaxation on approach to the p -wave Feshbach resonance is much smaller than in the three-dimensional (3D) case. This effect is mostly related to a much weaker enhancement of the relative wavefunction near the resonance in reduced dimensionalities. We then demonstrate this for the case of ^{40}K atoms in the $9/2$, $-7/2$ state.

II. 2-BODY INELASTIC COLLISIONS IN 3D

Let us consider two colliding identical fermions in the vicinity of a p -wave Feshbach resonance. In the single-channel model the radial wavefunction of their p -wave relative motion at distances $r \gg R_e$, where R_e is a characteristic radius of interaction, has the following form [14]:

$$\psi_{3D}(r) = i \{j_1(kr) + ikf(k)h_1(kr)\}, \quad (1)$$

where k is the relative momentum, $j_1(kr)$ and $h_1(kr)$ are spherical Bessel and Hankel functions, and $f(k)$ is the

p -wave scattering amplitude, which is related to the scattering phase shift $\delta(k)$ as $f(k) = 1/[k(\cot \delta(k) - i)]$. The p -wave S-matrix element is given by $S(k) = \exp 2i\delta(k)$. It is convenient to write the wavefunction (1) at $r \rightarrow \infty$ as $\psi_{3D} = (1/2ikr) \{\exp(-ikr) + S(k) \exp(ikr)\}$. In the presence of inelastic collisions the intensity of the outgoing wave is reduced in comparison to the incoming wave by a factor of $|S(k)|^2 < 1$, which implies that the phase shift $\delta(k)$ is a complex quantity with a positive imaginary part. For low collisional energies $E = \hbar^2 k^2/m$ we can use the effective range expansion $k^3 \cot \delta(k) = -1/w_1 - \alpha_1 k^2$, where w_1 is the scattering volume and $\alpha_1 > 0$ is the effective range. Then, the scattering amplitude becomes

$$f(k) = \frac{-k^2}{1/w_1 + \alpha_1 k^2 + ik^3}, \quad (2)$$

and in order to describe inelastic collisions in the vicinity of the resonance, we add an imaginary part to the inverse of the scattering volume: $1/w_1 \rightarrow 1/w_1 + i/w'_1$, where $w'_1 > 0$. Therefore, the S-matrix element reads

$$S(k) = \frac{1/w_1 + \alpha_1 k^2 + i(1/w'_1 - k^3)}{1/w_1 + \alpha_1 k^2 + i(1/w'_1 + k^3)}. \quad (3)$$

For the inelastic rate constant $\alpha_{3D}(k) = v\sigma_{3D}^{\text{in}}(k)$, where $v = 2\hbar k/m$ is the relative velocity and $\sigma_{3D}^{\text{in}}(k) = 3\pi [1 - |S(k)|^2]/k^2$ is the p -wave inelastic scattering cross-section [14], we obtain:

$$\alpha_{3D}(k) = \frac{48\pi\hbar}{mw'_1} \frac{k^2}{[1/w_1 + \alpha_1 k^2]^2 + [1/w'_1 + k^3]^2}, \quad (4)$$

where m is the atom mass and an additional factor of 2 is included since we consider collisions of identical particles.

Sufficiently far from resonance, where the dominant term in the denominator of Eq. (4) is $1/w_1$, the rate constant becomes

$$\alpha_{3D}(k) \approx \frac{48\pi\hbar}{m} \frac{w_1^2}{w'_1} k^2. \quad (5)$$

At $T = 0$ we average the rate constant over the Fermi step momentum distribution, and in the off-resonant regime Eq. (5) yields

$$\langle \alpha_{3D} \rangle_0 \approx \frac{144\pi}{5} \frac{w_1^2}{w_1'} \frac{E_F^{3D}}{\hbar}, \quad (6)$$

where $E_F^{3D} = \hbar^2 k_F^2 / 2m$ is the Fermi energy, $k_F = (6\pi^2 n_{3D})^{1/3}$ is the Fermi momentum for a single-component 3D gas, and n_{3D} is the 3D density.

Near the resonance on its negative side ($w_1 < 0$) the largest contribution to the rate constant comes from momenta close to $\tilde{k}_{3D} = 1/\sqrt{\alpha_1 |w_1|}$. In the near-resonant regime, where $|w_1|(1/w_1' + \tilde{k}_{3D}^3) \ll 1$ and $\tilde{k}_{3D} \ll k_F$, the rate constant exhibits a sharp peak, which is slightly shifted with respect to the position of the resonance at zero kinetic energy ($1/w_1 = 0$). The maximum value of the rate constant can be estimated as

$$\langle \alpha_{3D} \rangle_0 \approx \frac{576\pi^2 \hbar}{\alpha_1 m} \frac{1}{1 + w_1' \tilde{k}_{3D}^3} \left(\frac{\tilde{k}_{3D}}{k_F} \right)^3. \quad (7)$$

The results of direct numerical calculation of $\langle \alpha_{3D} \rangle_0$ for ^{40}K atoms are presented in Fig. 1 for $E_F^{3D} = 1 \mu\text{K}$ and $4 \mu\text{K}$ (corresponding to densities $n_{3D} \approx 3.6 \times 10^{13} \text{ cm}^{-3}$ and $2.9 \times 10^{14} \text{ cm}^{-3}$, respectively). In order to determine w_1' we fit Eq. (4) to the results of coupled-channel numerical calculations of the relaxation rate for a gas of ^{40}K atoms in $9/2, -7/2$ state at a fixed collisional energy of $1 \mu\text{K}$ [15], using the values of w_1 and α_1 that have been measured in the JILA experiment [9]. Then we obtain $w_1' = 0.53 \times 10^{-12} \text{ cm}^3$. The off-resonant expression (6) shows perfect agreement with the numerical results, and the near-resonant expression (7) leads to a slight overestimate. However, Eq. (7) correctly captures that in the vicinity of the maximum $\langle \alpha_{3D} \rangle_0 \sim (E_F^{3D})^{-3/2}$, in contrast to the off-resonant case, where the rate constant behaves as $\langle \alpha_{3D} \rangle_0 \sim E_F^{3D}$.

For the classical gas ($T \gg E_F^{3D}$) averaging $\alpha_{3D}(k)$ over the Boltzmann distribution of atoms, in the off-resonant regime we obtain:

$$\langle \alpha_{3D} \rangle_T \approx \frac{72\pi w_1^2}{w_1'} \frac{T}{\hbar}. \quad (8)$$

On the negative side of the resonance in the near-resonant regime, where $|w_1|(1/w_1' + \tilde{k}_{3D}^3) \ll 1$ and $\tilde{k}_{3D} \ll k_T$, with $k_T = \sqrt{mT/\hbar^2}$ being the thermal momentum, the rate constant has a sharp peak slightly shifted with

respect to the resonance at zero kinetic energy:

$$\langle \alpha_{3D} \rangle_T = \frac{96\pi^{3/2} \hbar}{\alpha_1 m} \frac{1}{1 + w_1' \tilde{k}_{3D}^3} \left(\frac{\tilde{k}_{3D}}{k_T} \right)^3. \quad (9)$$

Direct numerical calculation of $\langle \alpha_{3D} \rangle_T$ shows a perfect agreement with both off-resonant and near-resonant expressions, as shown in Fig. 2 for $T = 300 \text{ nK}$ and $T = 1 \mu\text{K}$.

Thus, we see that the inelastic rate constant has a drastically different temperature (Fermi energy) dependence in the near-resonant regime compared to the off-resonant case. For deep inelastic collisions the energy dependence of the rate constant is completely determined by the wavefunction of the initial state of colliding particles. In order to gain insight into the behavior of the inelastic rate constant we analyze the behavior of the wavefunction of the relative motion of two atoms at distances where $R_e \ll r \ll k^{-1}$. Using Eq. (1) and the expressions for the amplitude $f(k)$ and the phase shift $\delta(k)$ written after this equation, we have:

$$\psi_{3D}(r) \approx i \frac{(1/w_1 + \alpha_1 k^2) kr/3 - k/r^2}{1/w_1 + \alpha_1 k^2 + ik^3}. \quad (10)$$

In the off-resonant regime the terms containing $1/w_1$ are the leading ones in both the numerator and denominator of Eq. (10), and $\psi_{3D}^{\text{off}} \approx ikr/3$. This leads to $\alpha_{3D}^{\text{off}}(k) \sim k^2$, in agreement with Eq. (5). In the off-resonant regime collisions with all momenta in the distribution function contribute to the inelastic rate constant. In contrast, in the near-resonant regime on the negative side of the resonance ($w_1 < 0$) only a small fraction of relative momenta contributes to α_{3D} . These are momenta in a narrow interval $\delta k \sim \tilde{k}_{3D}^2/\alpha_1$ around \tilde{k}_{3D} . Accordingly, in the classical gas the fraction of such momenta is $F_{3D} \sim \tilde{k}_{3D}^2 \delta k / k_T^3 \sim \tilde{k}_{3D}^4 / (\alpha_1 k_T^3)$. In this near-resonant regime we have $|1/w_1 + \alpha_1 k^2| \sim \tilde{k}_{3D}^3$. Then, putting the rest of k 's equal to \tilde{k}_{3D} in Eq. (10) and taking into account that $\tilde{k}_{3D} r \ll 1$ at r approaching R_e , we see that the relative wavefunction in the near-resonant regime is $\psi_{3D}^{\text{res}} \approx 1/(\tilde{k}_{3D} r)^2$. The ratio of the near-resonant inelastic rate constant to the off-resonant one is $\mathcal{R}_{3D} \sim (\psi_{3D}^{\text{res}}/\psi_{3D}^{\text{off}})^2 F_{3D}$, where we have to put $r \sim R_e$ in the expressions for the relative wavefunctions. This yields

$$\mathcal{R}_{3D} \equiv \langle \alpha_{3D}^{\text{res}} \rangle_T / \langle \alpha_{3D}^{\text{off}} \rangle_T \sim 1/(k_T R_e)^5. \quad (11)$$

This is consistent with equations (8) and (9), since $\alpha_1 \sim 1/R_e$ and w_1 in the off-resonant regime is $\sim R_e^3$ (and we may omit unity compared to $w_1' \tilde{k}_{3D}^3$ in the denominator of (9)).

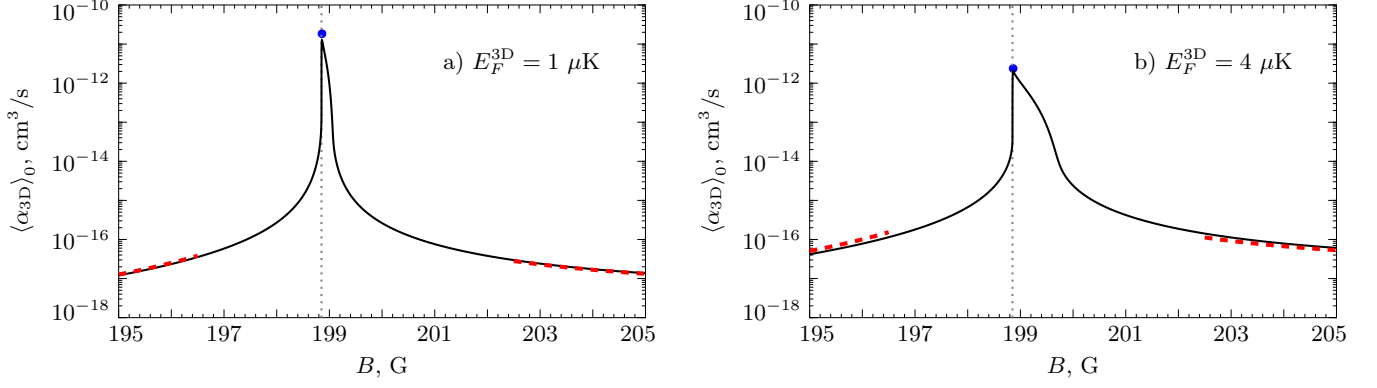


FIG. 1. Three-dimensional inelastic rate constant $\langle \alpha_{3D} \rangle_0$ for ^{40}K atoms in the $9/2, -7/2$ state at $T = 0$ versus magnetic field B for $E_F^{3D} = 1 \mu\text{K}$ in a) and $E_F^{3D} = 4 \mu\text{K}$ in b). Dashed red curves correspond to the off-resonant regime described by Eq. (6), the blue point marks the near-resonant peak value given by Eq. (7), and the grey vertical dotted line shows the magnetic field B_0 at which the scattering volume w_1 diverges.

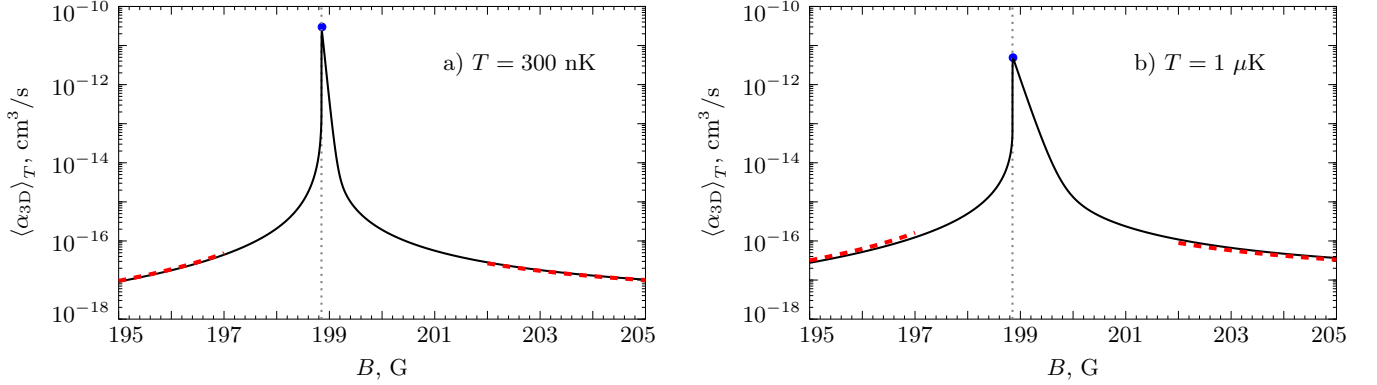


FIG. 2. Three-dimensional inelastic rate constant $\langle \alpha_{3D} \rangle_T$ for ^{40}K atoms in the $9/2, -7/2$ state versus magnetic field B for $T = 300 \text{ nK}$ in a) and $T = 1 \mu\text{K}$ in b). Dashed red curves correspond to the off-resonant regime described by Eq. (8), the blue point marks the near-resonant peak value according to Eq. (9), and the grey vertical dotted line shows the magnetic field B_0 at which the 3D scattering volume w_1 diverges.

III. 2-BODY INELASTIC COLLISIONS IN 2D

In the quasi-2D geometry obtained by a tight harmonic confinement in the axial direction (z) with frequency ω_0 , at in-plane (x, y) interatomic separations ρ greatly exceeding the extension of the wavefunction in the axial direction, $l_0 = (\hbar/m\omega_0)^{1/2}$, the p -wave relative motion is described by the wavefunction

$$\psi_{2D}(\mathbf{r}) = \varphi_{2D}(\rho) e^{i\vartheta} \frac{1}{(2\pi l_0^2)^{1/4}} \exp\left\{-\frac{z^2}{4l_0^2}\right\}; \quad \rho \gg l_0, \quad (12)$$

where ϑ is the scattering angle, and z is the interparticle separation in the axial direction. For remaining in the ultracold limit with respect to the axial motion we will assume below that $l_0 \gg R_e$ [17]. Then the 2D p -wave

radial wavefunction φ_{2D} is

$$\varphi_{2D}(\rho) = i \left\{ J_1(q\rho) - \frac{i}{4} f_{2D}(q) H_1(q\rho) \right\}, \quad (13)$$

with q being the 2D relative momentum, and $J_1(q\rho)$ and $H_1(q\rho)$ the Bessel and Hankel functions. The p -wave quasi-2D scattering amplitude $f_{2D}(q)$ is given by [16]

$$f_{2D}(q) = \frac{4q^2}{1/A_p + B_p q^2 - (2q^2/\pi) \ln l_0 q + i q^2}, \quad (14)$$

where the 2D scattering parameters are $1/A_p = (4/3\sqrt{2\pi}l_0^2) [l_0^3/w_1 - C_1]$ and $B_p = (4/3\sqrt{2\pi}) [l_0\alpha_1 - C_2]$, with numerical constants $C_1 \approx 6.5553 \times 10^{-2}$ and $C_2 \approx 1.4641 \times 10^{-1}$. The amplitude f_{2D} is related to the S-matrix element S_{2D} as $f_{2D}(q) = 2i(S_{2D}(q) - 1)$. The

2D (confinement-induced) resonance occurs at $1/A_p = 0$ and is thus shifted with respect to the 3D resonance ($1/w_1 = 0$). Like in the 3D case, in the presence of inelastic processes we have to replace $1/w_1$ by $1/w_1 + i/w'_1$, which yields

$$S_{2D}(q) = \frac{\frac{1}{A_p} + \left(B_p - \frac{2 \ln l_0 q}{\pi}\right) q^2 + i \left(\frac{1}{A'_p} - q^2\right)}{\frac{1}{A_p} + \left(B_p - \frac{2 \ln l_0 q}{\pi}\right) q^2 + i \left(\frac{1}{A'_p} + q^2\right)}, \quad (15)$$

with $A'_p = 3\sqrt{2\pi}w'_1/4l_0 > 0$. Then, writing the wavefunction (13) at $\rho \rightarrow \infty$ as $\varphi_{2D} \approx (1/\sqrt{2\pi i q \rho}) \{\exp(-iq\rho) + iS_{2D}(q) \exp(iq\rho)\}$ we see that the intensity of the outgoing wave is reduced by a factor of $|S_{2D}(q)|^2 < 1$ compared to the incoming wave. The 2D inelastic cross-section is defined as $\sigma_{2D}^{\text{in}} = (2/q)(1 - |S_{2D}(q)|^2)$, and for identical particles one has an additional factor of 2. Then, for the inelastic rate constant, $\alpha_{2D}(q) = (2\hbar q/m)\sigma_{2D}^{\text{in}}$, we obtain:

$$\alpha_{2D}(q) = \frac{32\hbar}{m A'_p} \times \frac{q^2}{\left[\frac{1}{A_p} + \left(B_p - \frac{2 \ln l_0 q}{\pi}\right) q^2\right]^2 + \left[\frac{1}{A'_p} + q^2\right]^2}. \quad (16)$$

Sufficiently far from the resonance, where the dominant term in the denominator of Eq. (16) is $1/A_p$, the rate constant becomes

$$\alpha_{2D}(q) \approx \frac{32\hbar}{m} \frac{A_p^2}{A'_p} q^2 \approx \frac{24\sqrt{2\pi}\hbar w_1^2}{m l_0} \frac{q^2}{w'_1}. \quad (17)$$

At $T = 0$, averaging the off-resonant rate constant (17) over the Fermi step momentum distribution we obtain

$$\langle \alpha_{2D} \rangle_0 \approx \frac{12\sqrt{2\pi}w_1^2}{l_0 w'_1} \frac{E_F^{2D}}{\hbar}, \quad (18)$$

where $E_F^{2D} = \hbar^2 q_F^2/2m$ is the 2D Fermi energy, $q_F = \sqrt{4\pi n_{2D}}$ is the Fermi momentum for a single-component 2D gas, and n_{2D} is the 2D density.

Near the 2D resonance on its negative side ($A_p < 0$) the largest contribution to the rate constant comes from momenta close to $\tilde{q}_{2D} = 1/\sqrt{B_p|A_p|}$. Then, in the regime, where $(A'_p)^{-1/2} \ll \tilde{q}_{2D} \ll q_F$, the rate constant has a sharp peak. The maximum value of the 2D rate constant at $T = 0$ can then be estimated as

$$\langle \alpha_{2D} \rangle_0 \approx \frac{128\pi\hbar}{A'_p B_p m} \frac{1}{q_F^2} \approx \frac{128\pi\hbar}{\alpha_1 m w'_1} \frac{1}{q_F^2}, \quad (19)$$

where we took into account that $A'_p B_p = w'_1(\alpha_1 l_0 - C_2)/l_0 \approx w'_1 \alpha_1$ for typical confinement frequencies ω_0 from 50 to 150 kHz. Therefore, the tight harmonic confinement has almost no influence on the maximum value of $\langle \alpha_{2D} \rangle_0$.

The results of direct numerical calculation of $\langle \alpha_{2D} \rangle_0$ for ^{40}K atoms are presented in Fig. 3 for the confining frequency $\omega_0 = 120$ kHz and Fermi energies $E_F^{2D} = 1$ μK and 4 μK (corresponding to densities $n_{2D} \approx 1.3 \times 10^9$ cm^{-2} and 5.2×10^9 cm^{-2} , respectively). The off-resonant expression (18) shows perfect agreement with the numerical results, while the near-resonant expression (19) leads to a slight overestimate. However, Eq. (19) captures that in the vicinity of the maximum $\langle \alpha_{2D} \rangle_0 \sim 1/E_F^{2D}$, in contrast to the off-resonant case, where $\langle \alpha_{2D} \rangle_0 \sim E_F^{2D}$.

At $T \gg E_F^{2D}$, we average Eq. (16) over the Boltzmann distribution of atoms. Then, the off-resonant expression for the rate constant follows from Eq. (17) and reads

$$\langle \alpha_{2D} \rangle_T \approx \frac{24\sqrt{2\pi}w_1^2}{l_0 w'_1} \frac{T}{\hbar}. \quad (20)$$

On the negative side of the 2D resonance in the near-resonant regime, where $(A'_p)^{-1/2} \ll \tilde{q}_{2D} \ll q_T$, with $q_T = \sqrt{mT/\hbar^2}$ being the thermal momentum, the rate constant has a sharp peak slightly shifted from the position of the 2D resonance at zero kinetic energy. The maximum value of the rate constant is given by

$$\langle \alpha_{2D} \rangle_T \approx \frac{32\pi\hbar}{A'_p B_p m} \frac{1}{q_T^2} \approx \frac{32\pi\hbar}{\alpha_1 m w'_1} \frac{1}{q_T^2}. \quad (21)$$

Like in the zero temperature case, we see that the maximum value of $\langle \alpha_{2D} \rangle_T$ is practically independent of the confinement frequency.

Direct numerical calculation of $\langle \alpha_{2D} \rangle_T$ shows perfect agreement with both off-resonant and near-resonant expressions, as displayed in Fig. 4 for the confining frequency $\omega_0 = 120$ kHz and temperatures $T = 300$ nK and $T = 1$ μK .

In order to qualitatively understand the temperature (Fermi energy) dependence of the inelastic rate constant, we analyze the structure of the initial state wavefunction which for deep inelastic processes fully determines the energy dependence of α_{2D} . Inelastic collisions occur at interparticle distances $r \lesssim R_e \ll l_0$, where the relative motion of colliding atoms has a three-dimensional character and ψ_{2D} is different from ψ_{3D} only by a normalization coefficient. Assuming the inequality $l_0 \ll k^{-1}$, at distances r exceeding R_e from Eq. (10) sufficiently far from the 3D resonance we have $\psi_{3D}(r) \propto \{r - 3w_1/r^2\}$. Then, according to Ref. [16], the 2D wavefunction can be written as

$$\psi_{2D}(r) = \frac{if_{2D}(q)(2\pi l_0^2)^{1/4}}{6\pi w_1 q} \{r - 3w_1/r^2\}. \quad (22)$$

Far from the 2D resonance ($1/A_p = 0$) the 2D scattering amplitude is $f_{2D}^{\text{off}} \approx 3\sqrt{2\pi}w_1 q^2/l_0$, which leads to $\psi_{2D}^{\text{off}} \sim (q/\sqrt{l_0}) \{r - 3w_1/r^2\}$ and $\alpha_{2D}^{\text{off}} \sim q^2/l_0$, in agreement with Eq. (17). In the near-resonant regime on the negative side of the 2D resonance ($A_p < 0$) the main contribution to α_{2D} is provided by relative momenta in a narrow interval $\delta q \sim \tilde{q}_{2D}/B_p$ around \tilde{q}_{2D} .

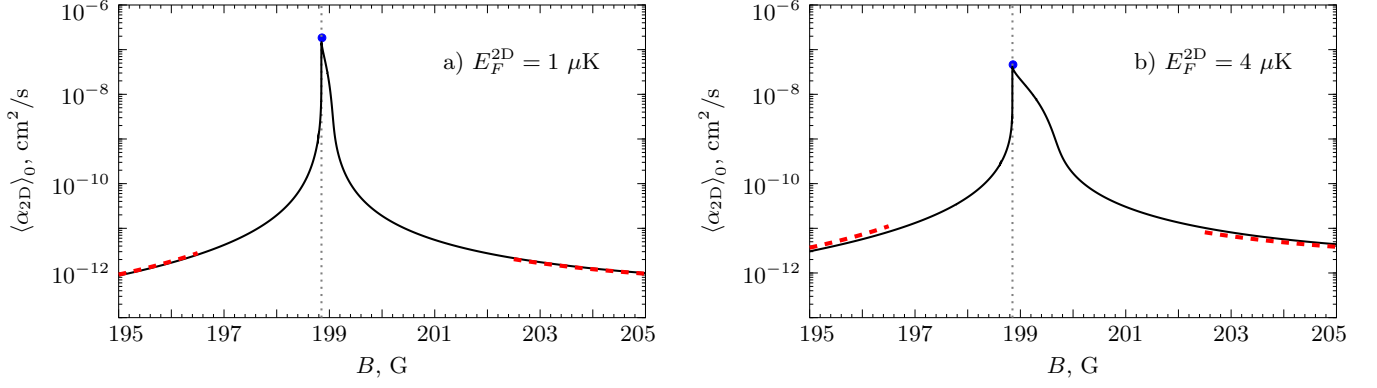


FIG. 3. Two-dimensional inelastic rate constant $\langle \alpha_{2D} \rangle_0$ for ^{40}K atoms in the $9/2, -7/2$ state at $T = 0$ versus magnetic field B for $E_F^{2D} = 1 \mu\text{K}$ in a) and $E_F^{2D} = 4 \mu\text{K}$ in b). Dashed red curves correspond to the off-resonant regime described by Eq. (18), the blue point marks the near-resonant peak value according to Eq. (19), and the grey vertical dotted line shows the magnetic field B_0 at which the 3D scattering volume w_1 diverges. The confining frequency is $\omega_0 = 120$ kHz.

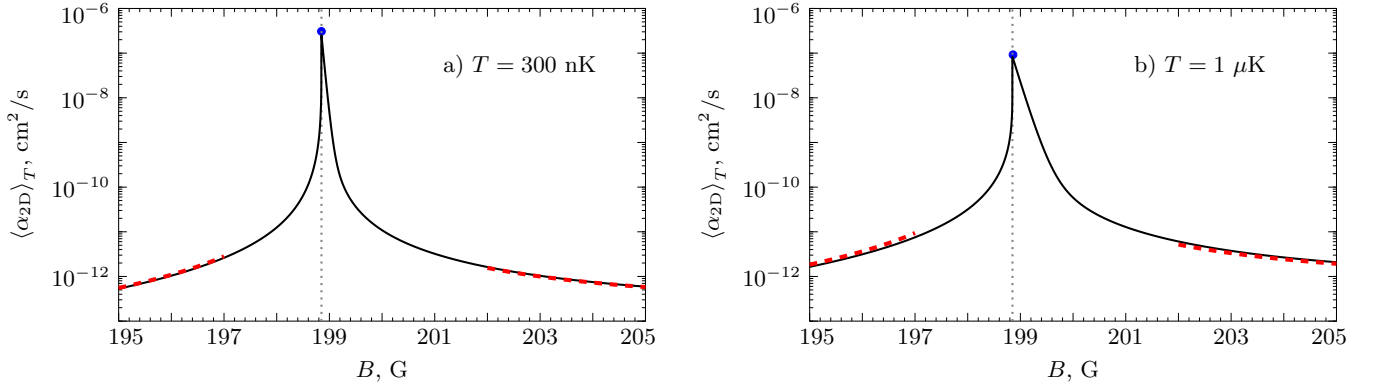


FIG. 4. Two-dimensional inelastic rate constant $\langle \alpha_{2D} \rangle_T$ for ^{40}K atoms in the $9/2, -7/2$ state versus magnetic field B for $T = 300$ nK in a) and $T = 1 \mu\text{K}$ in b). Dashed red curves correspond to the off-resonant regime described by Eq. (20), the blue point marks the near-resonant peak value according to Eq. (21), and the grey vertical dotted line shows the magnetic field B_0 at which the 3D scattering volume w_1 diverges. The confining frequency is $\omega_0 = 120$ kHz.

In the classical gas the fraction of such momenta is $F_{2D} \sim \tilde{q}_{2D} \delta q / q_T^2 \sim \tilde{q}_{2D}^2 / (B_p q_T^2)$. In this near-resonant regime we have $|1/A_p + B_p q^2| \sim \tilde{q}_{2D}^2$. Then, we may put the rest of q 's equal to \tilde{q}_{2D} in Eq. (22) and use $f_{2D}^{\text{res}}(q) \approx -4i$ (omitting the logarithmic term in the denominator of $f_{2D}(q)$). Thus, the 2D wavefunction becomes $\psi_{2D}^{\text{res}} \sim (\sqrt{l_0}/\tilde{q}_{2D}) \{r/w_1 - 3/r^2\}$. The ratio of the near-resonant inelastic rate constant to the off-resonant one is $\mathcal{R}_{2D} \sim (\psi_{2D}^{\text{res}}/\psi_{2D}^{\text{off}})^2 F_{2D}$, where we have to put $r \sim R_e$ in the expressions for the relative wavefunctions and take into account that in the off-resonant regime

$w_1 \sim R_e^3$ whereas in the near-resonant regime it is much larger. This yields [18]

$$\mathcal{R}_{2D} \equiv \langle \alpha_{2D}^{\text{res}} \rangle_T / \langle \alpha_{2D}^{\text{off}} \rangle_T \sim \frac{l_0}{R_e} \frac{1}{(q_T R_e)^4}, \quad (23)$$

which is consistent with equations (20) and (21). As one can see from Eqs. (11) and (23), the ratio $\mathcal{R}_{2D}/\mathcal{R}_{3D} \sim l_0 k_T \ll 1$. Thus, in 2D the enhancement of the inelastic rate constant near the resonance is much smaller than in 3D.

IV. 2-BODY INELASTIC COLLISIONS IN 1D

In the quasi-1D geometry obtained by a tight harmonic confinement in two directions (x, y) with frequency ω_0 ,

the wavefunction of the relative motion in the odd-wave

channel (analog of p -wave in 2D and 3D) is

$$\psi_{1D}(\mathbf{r}) = \chi_{1D}(z) \frac{1}{\sqrt{2\pi}l_0} \exp\left\{-\frac{\rho^2}{4l_0^2}\right\}, \quad (24)$$

where z is the longitudinal interparticle separation, $\rho = \sqrt{x^2 + y^2}$ is the transverse separation, and $l_0 = \sqrt{\hbar/(m\omega_0)}$ is the extension of the wavefunction in the (x, y) plane. The longitudinal motion with the 1D relative momentum q at distances $|z| \gg l_0 \gg R_e$ is described by the wavefunction

$$\chi_{1D}(z) = i \sin qz + \text{sgn}(z) f_{1D}(q) e^{iq|z|}, \quad (25)$$

with the odd-wave scattering amplitude $f_{1D}(q)$ given by [16]

$$f_{1D}(q) = \frac{-iq}{1/l_p + \xi_p q^2 + iq}, \quad (26)$$

where $l_p = 3l_0 [l_0^3/w_1 + 3\sqrt{2}|\zeta(-1/2)|]^{-1}$ and $\xi_p = \alpha_1 l_0^2/3$ are the 1D scattering parameters, and $\zeta(-1/2) \approx -0.208$ is the Riemann zeta-function. The amplitude $f_{1D}(k)$ is related to the 1D odd-wave S-matrix element $S_{1D}(q)$ as $f_{1D}(q) = (S_{1D}(q) - 1)/2$. Like in higher dimensions, in the presence of inelastic processes we should replace $1/w_1$ with $1/w_1 + i/w'_1$, which gives the following expression for the S-matrix element:

$$S_{1D}(q) = \frac{1/l_p + \xi_p q^2 + i(1/l'_p - q)}{1/l_p + \xi_p q^2 + i(1/l'_p + q)}, \quad (27)$$

where $1/l'_p = l_0^2/3w'_1 > 0$. Then, writing the wavefunction (25) at $|z| \rightarrow \infty$ as $\chi_{1D} = \text{sgn}(z)(1/2) \{-\exp(-iq|z|) + S_{1D}(q) \exp(iq|z|)\}$, we see that the intensity of the outgoing wave is reduced by a factor of $|S_{1D}(q)|^2 < 1$ compared to the incoming wave. The inelastic cross-section in 1D is defined as $\sigma_{1D}^{\text{in}} = (1 - |S_{1D}(q)|^2)/2$, and for identical particles there is an additional factor of 2. Then, for the inelastic rate constant, $\alpha_{1D}(q) = (2\hbar q/m)\sigma_{1D}^{\text{in}}$, we obtain:

$$\alpha_{1D}(q) = \frac{8\hbar}{ml'_p} \frac{q^2}{[1/l_p + \xi_p q^2]^2 + [1/l'_p + q]^2}. \quad (28)$$

Sufficiently far from the 1D resonance ($1/l_p = 0$), where the dominant term in the denominator of Eq. (28) is $1/l_p$, the rate constant becomes

$$\alpha_{1D}(q) \approx \frac{8\hbar}{m} \frac{l_p^2}{l'_p} q^2 \approx \frac{24\hbar}{m l_0^2} \frac{w_1^2}{w'_1} q^2. \quad (29)$$

At $T = 0$ the off-resonant rate constant averaged over the Fermi step momentum distribution reads

$$\langle \alpha_{1D} \rangle_0 \approx \frac{8w_1^2}{l_0^2 w'_1} \frac{E_F^{1D}}{\hbar}, \quad (30)$$

where $E_F^{1D} = \hbar^2 q_F^2/2m$ is the 1D Fermi energy, $q_F = \pi n_{1D}$ is the Fermi momentum for a single-component 1D gas and n_{1D} is the 1D density.

In the vicinity of the 1D resonance on its negative side ($l_p < 0$) the largest contribution to the rate constant comes from momenta $\sim \tilde{q}_{1D} = 1/\sqrt{\xi_p |l_p|}$. Then, in the near-resonant regime, where $1/l'_p \ll \tilde{q}_{1D} \ll q_F$, the rate constant shows a narrow peak with the value

$$\langle \alpha_{1D} \rangle_0 \approx \frac{8\pi\hbar}{l'_p \xi_p m} \frac{1}{q_F} = \frac{8\pi\hbar}{\alpha_1 m w'_1} \frac{1}{q_F}. \quad (31)$$

As in the 2D case, the maximum value of $\langle \alpha_{1D} \rangle_0$ is almost independent of the confinement frequency.

The results of direct numerical calculation of $\langle \alpha_{1D} \rangle_0$ for ^{40}K atoms are presented in Fig. 5 for the confining frequency $\omega_0 = 120$ kHz and Fermi energies $E_F^{1D} = 1$ μK and 4 μK (corresponds to densities $n_{1D} \approx 4.1 \times 10^4$ cm^{-1} and 8.2×10^4 cm^{-1} , respectively). The off-resonant expression (30) and near-resonant expression (31) agree with numerical results, although Eq.(31) leads to a small overestimate of $\langle \alpha_{1D} \rangle_0$.

At $T \gg E_F^{1D}$, averaging the rate constant over the Boltzmann distribution of atoms we obtain the following off-resonant expression:

$$\langle \alpha_{1D} \rangle_T \approx \frac{12w_1^2}{l_0^2 w'_1} \frac{T}{\hbar}. \quad (32)$$

On the negative side of the 1D resonance in the near-resonant regime, where $1/l'_p \ll \tilde{q}_{1D} \ll q_T$, with $q_T = \sqrt{mT/\hbar^2}$ being the thermal momentum, the rate constant displays a sharp peak, slightly shifted with respect to the position of the 1D resonance at zero kinetic energy ($1/l_p = 0$). The maximum value of the rate constant is

$$\langle \alpha_{1D} \rangle_T \approx \frac{4\sqrt{\pi}\hbar}{l'_p \xi_p m} \frac{1}{q_T} = \frac{4\sqrt{\pi}\hbar}{\alpha_1 m w'_1} \frac{1}{q_T}. \quad (33)$$

Direct numerical calculation of $\langle \alpha_{1D} \rangle_T$ shows good agreement with both off-resonant and near-resonant expressions, as shown in Fig. 6 for the confining frequency $\omega_0 = 120$ kHz and temperatures $T = 300$ nK and $T = 1$ μK . Note that in the vicinity of the peak value the rate constant is proportional to $1/\sqrt{T}$, while in the off-resonant regime it has a linear dependence on T .

We see that in 1D, as well as in higher dimensions, the temperature (Fermi energy) dependence of the inelastic rate constant in the near-resonant regime is very different from that in the off-resonant case. Similarly to the 2D case, at distances where the relaxation occurs ($R_e \lesssim r \ll l_0$), the 1D relative wavefunction ψ_{1D} has a 3D character and differs from the 3D wavefunction only by a normalization coefficient. Sufficiently far from the 3D resonance, assuming that r is still larger than R_e , the 1D wavefunction can be written as [16]

$$\psi_{1D}(r) = -\frac{f_{1D}(q)\sqrt{2\pi}l_0}{6\pi w_1} \{r - 3w_1/r^2\}. \quad (34)$$

Far from the 1D resonance ($1/l_p = 0$) the 1D scattering amplitude is $f_{1D}^{\text{off}} \approx -3iw_1 q/l_0^2$, which yields $\psi_{1D}^{\text{off}} \approx$

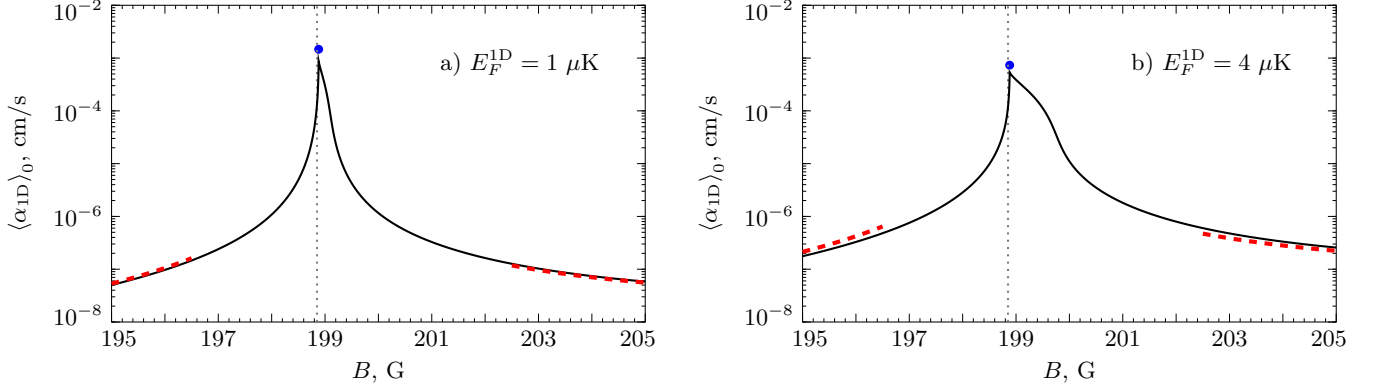


FIG. 5. One-dimensional inelastic rate constant $\langle \alpha_{1D} \rangle_0$ for ^{40}K atoms in the $9/2, -7/2$ state at $T = 0$ versus magnetic field B for $E_F^{1D} = 1 \mu\text{K}$ in a) and $E_F^{1D} = 4 \mu\text{K}$ in b). Dashed red curves correspond to the off-resonant regime described by Eq. (30), the blue point marks the near-resonant peak value according to Eq. (31), and the grey vertical dotted line shows the magnetic field B_0 at which the 3D scattering volume w_1 diverges. The confining frequency is $\omega_0 = 120$ kHz.

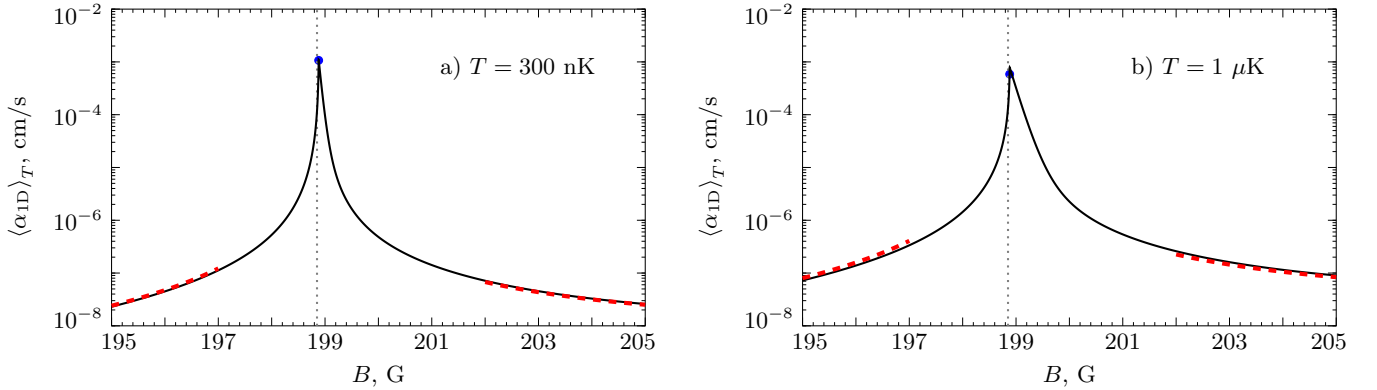


FIG. 6. One-dimensional inelastic rate constant $\langle \alpha_{1D} \rangle_T$ for ^{40}K atoms in the $9/2, -7/2$ state versus magnetic field B for $T = 300$ nK in a) and $T = 1 \mu\text{K}$ in b). Dashed red curves correspond to the off-resonant regime described by Eq. (32), the blue point marks the near-resonant peak value according to Eq. (33), and the grey vertical dotted line shows the magnetic field B_0 at which the 3D scattering volume w_1 diverges. The confining frequency is $\omega_0 = 120$ kHz.

$(iq/\sqrt{2\pi}l_0)\{r - 3w_1/r^2\}$ and $\alpha_{1D}^{\text{off}} \sim q^2/l_0^2$, in agreement with Eq. (29). In the near-resonant regime on the negative side of the confinement-induced resonance ($l_p < 0$) the situation changes. Here the main contribution to α_{1D} is provided only by relative momenta in a narrow interval $\delta q \sim 1/\xi_p$ around \tilde{q}_{1D} , and in the classical gas the fraction of such momenta is $F_{1D} \sim \delta q/q_T \sim 1/(\xi_p q_T)$. In this near-resonant regime we have $|1/l_p + \xi_p q^2| \sim \tilde{q}_{1D}$ and $f_{1D}^{\text{res}}(q) \approx -1$. Then, the 1D wavefunction becomes $\psi_{1D}^{\text{res}} \sim l_0 \{r/w_1 - 3/r^2\}$. The ratio of the near-resonant inelastic rate constant to the off-resonant one is $\mathcal{R}_{1D} \sim (\psi_{1D}^{\text{res}}/\psi_{1D}^{\text{off}})^2 F_{1D}$, where we have to put $r \sim R_e$ in the expressions for the relative wavefunctions. Taking

into account that in the off-resonant regime $w_1 \sim R_e^3$ and in the near-resonant regime it is much larger, we obtain:

$$\mathcal{R}_{1D} \sim \left(\frac{l_0}{R_e}\right)^2 \frac{1}{(q_T R_e)^3}, \quad (35)$$

which is consistent with equations (32) and (33). From Eqs. (11), (23), and (35) we find that $\mathcal{R}_{1D}/\mathcal{R}_{3D} \sim (k_T l_0)^2 \sim (k_T l_0) \mathcal{R}_{2D}/\mathcal{R}_{3D}$. Thus, in the 1D case the enhancement of the inelastic rate near the resonance is even weaker than in 2D and certainly much weaker than in 3D.

V. 2-BODY INELASTIC RATE NEAR THE RESONANCE IN 2D AND 1D. CONCLUSIONS

In this section we analyze how the inelastic rate is enhanced on approach to the resonance in reduced dimen-

sionalities and conclude. In 3D the rate equation in-

cluding the 2-body relaxation is $dn_{3D}/dt = -\langle\alpha_{3D}\rangle n_{3D}^2$, where $\langle\alpha_{3D}\rangle$ is the 3D relaxation rate constant. In reduced dimensionalities, at least in the off-resonant regime, we may assume that the rate equation is the same as in the 3D gas, but with a Gaussian density profile in the tightly confined direction(s). Accordingly, in the quasi-2D case we have the density profile in the axial direction, $n_{3D} = (n_{2D}/\sqrt{\pi}l_0)\exp\{-z^2/l_0^2\}$, and in the quasi-1D regime the radial density profile is $n_{3D} = (n_{1D}/\pi l_0^2)\exp\{-\rho^2/l_0^2\}$. Therefore, integrating out the motion in the tightly confined direction(s), we see that in 2D and 1D the inelastic 2-body relaxation is characterized by the rate constants

$$\langle\tilde{\alpha}_{2D}\rangle \simeq \frac{\langle\alpha_{3D}\rangle}{\sqrt{2\pi}l_0}; \quad \langle\tilde{\alpha}_{1D}\rangle \simeq \frac{\langle\alpha_{3D}\rangle}{2\pi l_0^2}. \quad (36)$$

These expressions look like a natural extension of the 3D results to the quasi-2D and quasi-1D cases.

In Fig.7 and Fig.8 we present our numerical results for the ratios $\langle\alpha_{2D}\rangle_T/\langle\tilde{\alpha}_{2D}\rangle_T$ and $\langle\alpha_{1D}\rangle_T/\langle\tilde{\alpha}_{1D}\rangle_T$ versus the magnetic field for ^{40}K atoms in the $9/2, -7/2$ state at $T = 300$ nK and $T = 1$ μK . As expected, far from

the resonances these ratios are of order unity (according to Eqs. (8), (20), and (32) they are $2/3$ in 2D and $1/3$ in 1D). However, on approach to the resonance (where the rate constant by itself grows) they strongly decrease [19]. This simply means that the enhancement of the 2-body inelastic rate near the resonance is much weaker in reduced dimensionalities than in 3D. The effect is especially pronounced in 1D, which is consistent with our discussion in the previous section.

This effect is mostly related to a weaker enhancement of the relative wavefunction on approach to the resonance in 2D and 1D than in 3D. Indeed, using expressions for ψ_{3D} and ψ_{2D} in the near- and off-resonant regimes (written after Eqs. (10) and (22)) we see that the ratio $(\psi_{2D}^{\text{res}}/\psi_{2D}^{\text{off}})^2/(\psi_{3D}^{\text{res}}/\psi_{3D}^{\text{off}})^2 \sim (\tilde{k}_{3D}l_0)^2 \ll 1$ slightly away from the 3D resonance. Similarly, in 1D we have $(\psi_{1D}^{\text{res}}/\psi_{1D}^{\text{off}})^2/(\psi_{3D}^{\text{res}}/\psi_{3D}^{\text{off}})^2 \sim (\tilde{k}_{3D}l_0)^4$, which is even smaller than in the 2D case.

Our results may draw promising paths to obtain novel many-body states in 2D and 1D, such as low density p -wave (odd-wave) superfluids of spinless fermions. It is quite likely that they can be extended to the case of three-body recombination [20], which will be the topic of our future research.

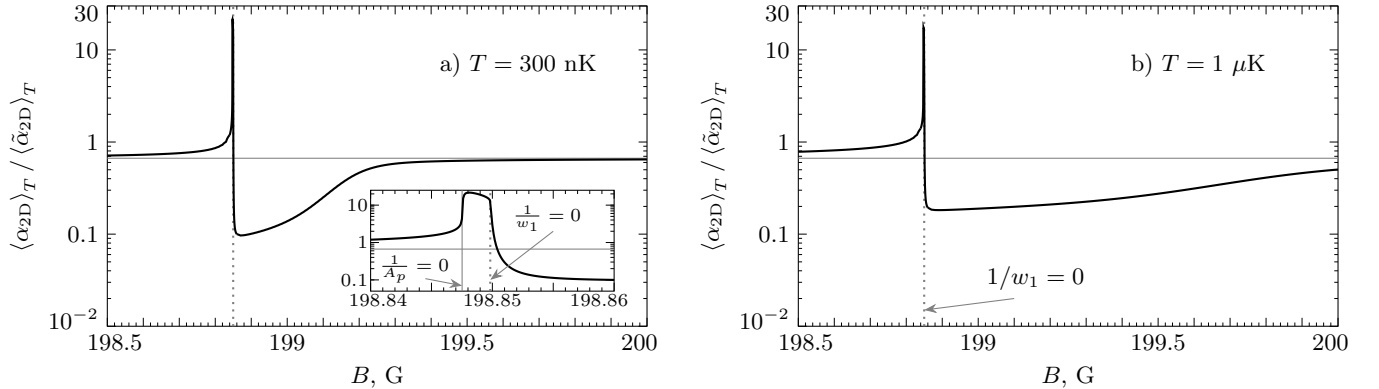


FIG. 7. The ratio $\langle\alpha_{2D}\rangle_T/\langle\tilde{\alpha}_{2D}\rangle_T$ for ^{40}K atoms in the $9/2, -7/2$ state as a function of magnetic field B at $\omega_0 = 120$ kHz for $T = 300$ nK in a) and $T = 1$ μK in b). The solid grey horizontal line indicates the off-resonant value $\langle\alpha_{2D}\rangle_T/\langle\tilde{\alpha}_{2D}\rangle_T = 2/3$, and the grey dotted vertical line shows the value of magnetic field B_0 at which $1/w_1 = 0$. The inset in a) illustrates that $\langle\alpha_{2D}\rangle_T/\langle\tilde{\alpha}_{2D}\rangle_T$ significantly increases in a very narrow interval of magnetic fields $B_0^{2D} \lesssim B \lesssim B_0$, where B_0^{2D} is the field value at which $1/A_p = 0$ (shown by the grey solid vertical line).

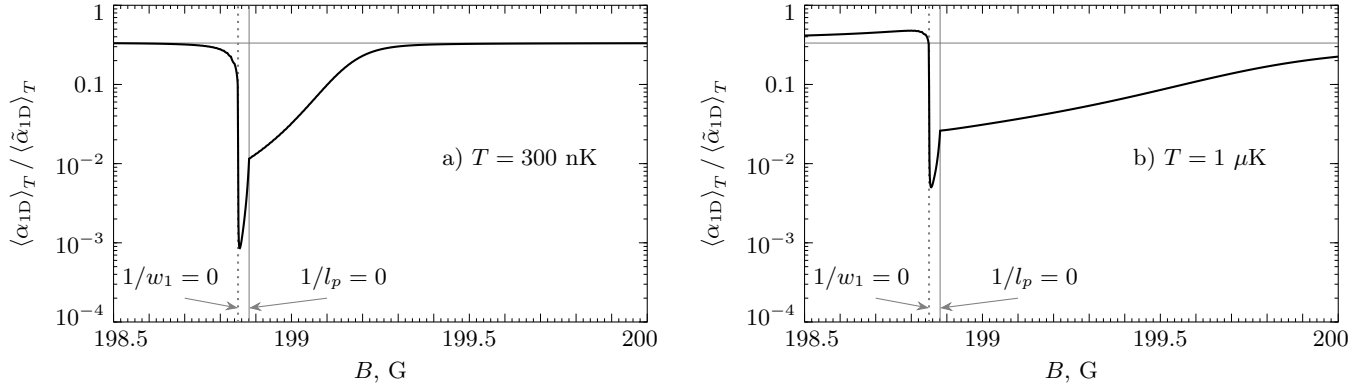


FIG. 8. The ratio $\langle \alpha_{1D} \rangle_T / \langle \tilde{\alpha}_{1D} \rangle_T$ for ^{40}K atoms in the $9/2, -7/2$ state as a function of magnetic field B at $\omega_0 = 120$ kHz for $T = 300$ nK in a) and $T = 1$ μK in b). The solid grey horizontal line indicates the off-resonant value $\langle \alpha_{1D} \rangle_T / \langle \tilde{\alpha}_{1D} \rangle_T = 1/3$, the grey dotted vertical line shows the magnetic field B_0 at which $1/w_1 = 0$, and the grey solid vertical line – the magnetic field B_0^{1D} at which $1/l_p = 0$.

ACKNOWLEDGMENTS

We would like to thank D. Petrov and A. Fedorov for useful discussions and J. Bohn for providing us with the results of coupled-channel numerical calculations. We acknowledge support from IFRAF and from the Dutch

Foundation FOM. The research leading to these results has received funding from the European Research Council under European Community's Seventh Framework Programme (FR7/2007-2013 Grant Agreement no. 341197).

-
- [1] V. Gurarie and L. Radzihovsky, *Ann. Phys. (Amsterdam)* **322**, 2 (2007).
 - [2] C. Nayak, S.H. Simon, A. Stern, M. Freedman, and S. Das Sarma, *Rev. Mod. Phys.* **80**, 1083 (2008).
 - [3] A. Stern, *Ann. Phys.* **323**, 204 (2008).
 - [4] C. Sanner, E. J. Su, W. Huang, A. Keshet, J. Gillen, and W. Ketterle, *Phys. Rev. Lett.* **108**, 240404 (2012).
 - [5] D. Pekker, M. Babadi, R. Sensarma, N. Zinner, L. Pollet, M.W. Zwierlein, and E. Demler, *Phys. Rev. Lett.* **106**, 050402 (2011).
 - [6] Y. Jiang, D.V. Kurlov, X.-W. Guan, F. Schreck, and G.V. Shlyapnikov, *Phys. Rev. A* **94**, 011601(R) (2016).
 - [7] L. Yang, X.-W. Guan, and X. Cui, *Phys. Rev. A* **93**, 051605(R) (2016).
 - [8] C. A. Regal, C. Ticknor, J. L. Bohn, and D. S. Jin, *Phys. Rev. Lett.* **90**, 053201 (2003).
 - [9] C. Ticknor, C. A. Regal, D. S. Jin, and J. L. Bohn, *Phys. Rev. A* **69**, 042712 (2004).
 - [10] F. Chevy, E. G. M. van Kempen, T. Bourdel, J. Zhang, L. Khaykovich, M. Teichmann, L. Tarruell, S. J. J. M. F. Kokkelmans, and C. Salomon, *Phys. Rev. A* **71**, 062710 (2005).
 - [11] J. P. Gaebler, J. T. Stewart, J. L. Bohn, and D. S. Jin, *Phys. Rev. Lett.* **98**, 200403 (2007).
 - [12] J. Levinsen, N.R. Cooper, and V. Gurarie, *Phys. Rev. A* **78**, 063616 (2008).
 - [13] M. Jona-Lasinio, L. Pricoupenko, and Y. Castin, *Phys. Rev. A* **77**, 043611 (2008).
 - [14] L.D. Landau and E.M. Lifshitz, *Quantum Mechanics, Non-Relativistic Theory* (Butterworth-Heinemann, Oxford, 1999).
 - [15] J. Bohn (private communication).
 - [16] L. Pricoupenko, *Phys. Rev. Lett.* **100**, 170404 (2008).
 - [17] D.S. Petrov and G.V. Shlyapnikov, *Phys. Rev. A* **64**, 014706 (2001).
 - [18] The quantity \mathcal{R}_{2D} remains the same if in the near-resonant regime (at $A_p < 0$) we are fairly close to the 3D resonance.
 - [19] As seen in Fig. 7, in the quasi-2D case there is a narrow region of magnetic fields where the ratio $\langle \alpha_{2D} \rangle_T / \langle \tilde{\alpha}_{2D} \rangle_T$ increases by an order of magnitude compared to its off-resonant value. The reason is that the position of the 2D resonance is slightly shifted to the positive side of the 3D resonance (the condition of the 2D resonance, $1/A_p = 0$, requires $w_1 = l_0^3/C_1 > 0$). Hence, for the field values between B_0 and B_0^{2D} one has $w_1 > 0$ and $A_p < 0$, and the 2D rate constant experiences much stronger enhancement than the 3D one. In contrast, the 1D resonance is shifted to the negative side of the 3D resonance, so that the ratio $\langle \alpha_{1D} \rangle_T / \langle \tilde{\alpha}_{1D} \rangle_T$ never exceeds unity.
 - [20] In 1D one has an extra suppression of 3-body recombination of identical fermions in the off-resonant regime by a factor of (E_F^{1D}/E_*) at $T = 0$ and (T/E_*) in the classical gas, where $E_* \sim 1$ mK is a characteristic molecular energy. For typical densities/temperatures this is about 3 orders of magnitude: B.D. Esry, H. Suno, and C.H. Greene, *The Expanding Frontier of Atomic Physics (ICAP-2002)* (World Scientific, Singapore, 2003); N.P.

Mehta, B.D. Esry, and C.H. Greene, [Phys. Rev. A **76**, 022711 \(2007\)](#).